Electrical and chemical synapses among parvalbumin fast-spiking GABAergic interneurons in adult mouse neocortex

Mario Galarreta*† and Shaul Hestrin*‡

Departments of *Comparative Medicine and ‡Neurology and Neurological Sciences, Stanford University School of Medicine, 300 Pasteur Drive, Edwards Building R102, Stanford, CA 94305-5330

Edited by Michael V. L. Bennett, Albert Einstein College of Medicine, Bronx, NY, and approved July 19, 2002 (received for review March 18, 2002)

Networks of γ-aminobutyric acid (GABA)ergic interneurons connected via electrical and chemical synapses are thought to play an important role in detecting and promoting synchronous activity in the cerebral cortex. Although the properties of electrical and chemical synaptic interactions among inhibitory interneurons are critical for their function as a network, they have only been studied systematically in juvenile animals. Here, we have used transgenic mice expressing the enhanced green fluorescent protein in cells containing parvalbumin (PV) to study the synaptic connectivity among fast-spiking (FS) cells in slices from adult animals (2–7 months old). We have recorded from pairs of PV-FS cells and found that the majority of them were electrically coupled (61%, 14 of 23 pairs). In addition, 78% of the pairs were connected via GABAergic chemical synapses, often reciprocally. The average coupling coefficient for step injections was 1.5% (n = 14), a smaller value than that reported in juvenile animals. GABA-mediated inhibitory postsynaptic currents and potentials decayed with exponential time constants of 2.6 and 5.9 ms, respectively, and exhibited paired-pulse depression (50-ms interval). The inhibitory synaptic responses in the adult were faster than those observed in young animals. Our results indicate that PV-FS cells are highly interconnected in the adult cerebral cortex by both electrical and chemical synapses, establishing networks that can have important implications for coordinating activity in cortical circuits.

Inhibitory γ-aminobutyric acid (GABA)ergic cells constitute ≈15–30% of neurons in the neocortex (1, 2). These cells can be classified into different types according to their physiology and histochemistry (3), their morphology and postsynaptic targets (4), and the presence of electrical synapses (5). The functional significance of this diversity and the characteristics of synaptic interactions of specific types of GABAergic neurons are only poorly understood.

Fast-spiking (FS) cells represent a well defined subgroup of prominent GABAergic interneurons that can be identified by their pattern of firing in response to current injection (3). Typically, FS cells generate discharges of high-frequency nonaccommodating spikes at near-threshold membrane potentials (6, 7). In addition, FS cells can be distinguished histochemically from other GABAergic interneurons by their selective expression of the calcium-binding protein parvalbumin (PV) (7–9). Morphologically, FS cells include both basket and chandelier cells and are located in every neocortical layer except layer I (6, 7, 9). These cells make somatic and proximal contacts onto neighboring pyramidal cells and are thought to exert a powerful inhibitory control on principal neurons (4).

In vivo (10–12) and *in vitro* (13, 14) experimental data, together with theoretical studies (15–19), suggest that networks of GABAergic interneurons play an important role in generating brain rhythms and synchronizing the activity of principal neurons. Although networks of FS cells are thought to operate in adult animals, the synaptic interactions among FS cells have only been studied systematically in juvenile tissue. By using slices from 2–4-week-old rats and mice, it has been demonstrated that FS cells can interact with each other via GABAergic as well as electrical synapses (refs. 7, 9, and 20–23; for review see ref. 5). In principle, both chemical and electrical connections could synchronize the activity within interneuron networks. Theoretical models have emphasized that the specific properties of these synapses including the degree of connectivity, the kinetics of the inhibitory postsynaptic currents (IPSCs), and the strength of the electrical coupling dramatically affect the function of these networks (15, 17, 19, 24). Whether functional electrical synapses exist in the cerebral cortex of adult animals and the characteristics of the GABA-mediated synaptic currents among FS cells in mature slices remain unknown.

To date, technical difficulties have prevented recording from pairs of visually identified interneurons in cortical slices from adult animals. Neurons are usually first selected based on the appearance of their somata and proximal processes under infrared videomicroscopy. When axonal myelination is completed, however, slices are much less transparent, and observing these features becomes extremely difficult. In this article, we used transgenic mice generated by Meyer *et al.* (25) containing the fluorescent marker enhanced GFP (EGFP) in cells expressing PV. By these means, we have recorded from pairs of FS cells in slices from adult animals and studied their functional synaptic interactions.

Materials and Methods

Slice Preparation and Cell Identification. Heterozygous C57BL/6 transgenic mice expressing EGFP under the control of the PV gene promoter (25) were cross-bred with ICR mice. Mice expressing the EGFP transgene were identified by detection of the characteristic fluorescence in skeletal muscle under UV illumination. Eighteen adult mice of both sexes (2–7 months old, mean 3.4 months, median 2.7 months) were anesthetized by an i.p. injection of ketamine (87 mg/kg) and xylazine (13 mg/kg) and decapitated. No apparent differences among animals within this age range were observed. Parasagittal cortical slices (300-μm thick, 30° angle) were obtained by using standard procedures. After dissection, the slices were incubated at 32–34°C for 30 min and then at room temperature (20–22°C) until transferred to a submersion-type recording chamber. The extracellular solution bathing the slices during the dissection, incubation, and recording contained 125 mM NaCl, 2.5 mM KCl, 1.25 mM NaH_2PO_4, 1 mM $MgSO_4$, 2 mM $CaCl_2$, 26 mM $NaHCO_3$, 20 mM glucose, 4 mM lactic acid, 2 mM pyruvic acid, and 0.4 mM ascorbic acid (pH 7.4, 315 milliosmol) and was bubbled continuously with a gas mixture of 95% O_2 and 5% CO_2.

This paper was submitted directly (Track II) to the PNAS office.

Abbreviations: GABA, γ-aminobutyric acid; FS, fast-spiking; PV, parvalbumin; IPSC, inhibitory postsynaptic current; EGFP, enhanced GFP; ISI, interspike interval; IPSP, inhibitory postsynaptic potential; $GABA_A$, GABA type A.

†To whom reprint requests should be addressed. E-mail: galarreta@stanford.edu.

www.pnas.org/cgi/doi/10.1073/pnas.192159599

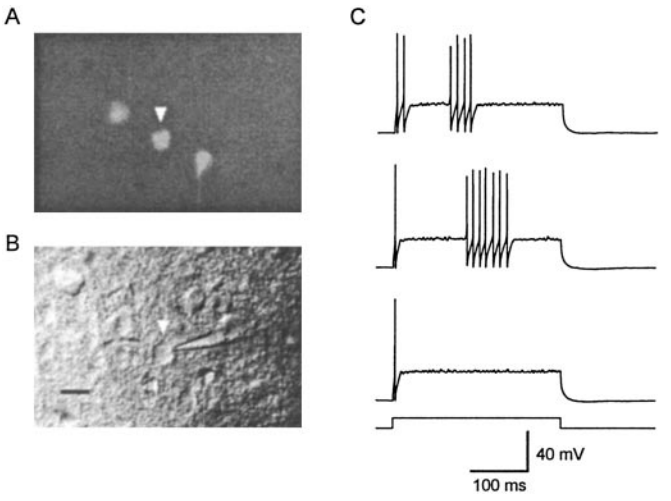

Fig. 1. Identification of PV-expressing neurons in adult neocortical slices. (*A*) Fluorescing cells in a neocortical slice obtained from a 2-month-old PV-EGFP-expressing mouse. Three EGFP-expressing neurons are illustrated. (*B*) same field under differential interference contrast infrared videomicroscopy. Note the tip of the patch electrode used to record the activity of an EGFP-expressing neuron. (Scale bar, 10 μm.) (*C*) Firing pattern in response to current injection (190 pA, 300 ms) of the EGFP-expressing neuron illustrated in *A* and *B* (arrowhead). The three responses were obtained with the same current injection. Note the discharges of high-frequency nonaccommodating action potentials in the two upper traces.

Kynurenic acid (1 mM) was added during the dissection and incubation period.

Fluorescent neurons in the somatosensory cortex were visualized by using an upright microscope (Axioskop, Zeiss) illuminated with a xenon lamp (150 W, OptiQuip, Highland Mills, NY) and equipped with a ×40 water-immersion lens and EGFP filters (XF100, Omega Optical, Brattleboro, VT). Once a fluorescent neuron was selected, it was visualized with infrared differential interference contrast video microscopy and recorded with conventional patch-clamp techniques (Fig. 1 *A* and *B*).

Paired Recordings and Data Analysis. Simultaneous somatic whole-cell recordings from pairs of PV-FS cells were made with patch electrodes (3–4 mΩ) filled with a solution containing 130 mM K-methylsulfate, 6.3 mM KCl, 10 mM Hepes, 4 mM MgATP, 20 mM phosphocreatine(Na), 0.3 mM NaGTP, 0.2 mM EGTA, and 0.3% biocytin (pH 7.3, 295 milliosmol). Liquid-junction potential error was not corrected. Recordings were performed at 32–34°C. In most experiments both cells were recorded under current-clamp mode. In others, the postsynaptic cell was kept under voltage-clamp mode. Signals were recorded with two Axopatch 200B patch clamps (Axon Instruments, Foster City, CA). The voltage and current output were filtered at 5 kHz and digitized at 16-bit resolution (ITC-18, Instrutech, Mineola, NY) with a sampling frequency of 10 kHz.

The input resistance and membrane time constant of PV-FS cells were calculated by injecting long pulses of depolarizing current (50 pA, 300 ms). Spike amplitude and the after-hyperpolarization potential were measured relative to the spike threshold. Spike-frequency adaptation was calculated as the ratio of the second to the first interspike intervals (ISIs) in near-threshold discharges of three or more action potentials. The strength of the electrical coupling in pairs of PV-FS cells is reported as the mean of the coupling coefficient between cell 1 and cell 2 and that measured between cell 2 and cell 1. The spike-coupling coefficient was calculated as the ratio of the area of the spikelet above the baseline to the area of the presynaptic spike above the threshold. Assuming a simple model of two isopotential neurons connected by a single electrical junction, the gap-junction conductance (Gc) was calculated according to the equation $Gc = 1/[(R_{in2}/CC) - R_{in2}]$, where R_{in2} is the input resistance of the postsynaptic neuron, and CC is the step-coupling coefficient. Complexities regarding the location of gap junctions in dendrites were not taken into account.

Data are given as mean ± SEM. Differences were considered statistically significant (Student's t test) if $P < 0.05$.

Results

Characterization of EGFP-Expressing Cells. All experiments have been performed in acute slices obtained from adult (2–7-month-old) transgenic mice, in which PV neurons expressed EGFP (25). In the neocortex, 94% of the EGFP-expressing cells contained PV (25). We first characterized the physiology of EGFP-expressing cells identified with fluorescent microscopy (Fig. 1*A*). We mainly selected neurons located in layer V; however, some cells in layers IV and II/III also were included in our study. Selected fluorescent neurons were visualized under IR-differential interference contrast video microscopy and recorded by using somatic whole-cell recordings (Fig. 1*B*). Most EGFP-positive cells showed the characteristic firing pattern of FS cells in response to pulses of depolarizing current (93%, 82 of 88 neurons). In response to near-threshold current injections, fluorescent cells typically fired one or two initial spikes followed, at a variable latency, by a discharge of high-frequency nonaccommodating action potentials (Fig. 1*C*). In these characteristic discharges, the mean frequency was 228 ± 18 Hz, the mean ISI ranged between 2 and 13.4 ms, the coefficient of variation of the ISI was 0.086 ± 0.008, and the spike-frequency adaptation (2nd ISI/1st ISI) was 1.09 ± 0.02. In addition, EGFP-expressing cells ($n = 41$ neurons) had an average resting membrane potential of −72 ± 1 mV, a membrane time constant of 3.8 ± 0.2 ms, and an input resistance of 89.2 ± 2.9 MΩ. Their action potentials had a mean half-width of 0.35 ± 0.01 ms and an amplitude of 61 ± 2 mV and were followed by a single fast component after-hyperpolarization potential with a mean amplitude of 25.4 ± 0.6 mV. The small percentage of fluorescent neurons that did not show the physiological characteristics of FS cells was excluded from the study. To study the morphology of PV-EGFP cells, they were injected with biocytin followed by anatomical reconstruction ($n = 8$). We found that PV-EGFP cells was aspiny interneurons with relatively heterogeneous anatomy. Their somata appearance ranged from multipolar to bitufted, and their axon branched profusely in the vicinity of the somata or above them (Fig. 2*A*). Altogether, these results indicate that PV-EGFP transgenic mice are a useful tool to study the function of FS cells in the adult brain. Hereinafter, we will refer to PV-EGFP neurons with FS properties as PV-FS cells.

Electrical Synapses Between PV-FS Cells. To study functional synaptic interactions among PV-FS cells in adult animals, we recorded simultaneously from pairs of closely neighboring neurons (Fig. 2*A*). The average distance between their somata was 39.0 ± 4.2 μm (range 13–92 μm, $n = 23$). We tested the presence of electrical coupling by injecting pulses of subthreshold depolarizing or hyperpolarizing current into one of the cells and detecting a change in the membrane voltage of the noninjected neuron. We found that 61% of the pairs examined (14 of 23 pairs) were electrically coupled (Fig. 2*B* and Table 1). To estimate the strength of the electrical coupling we calculated the coupling coefficient in response to a step-current pulse by obtaining the ratio between the voltage change produced in the noninjected cell and that in the injected cell. The coupling coefficient ranged from 0.11% to 4.9% with an average value of 1.53% ± 0.34% ($n = 14$; Fig. 2*C*), and was similar for depolarizing or hyperpolarizing injections. Electrical coupling was al-

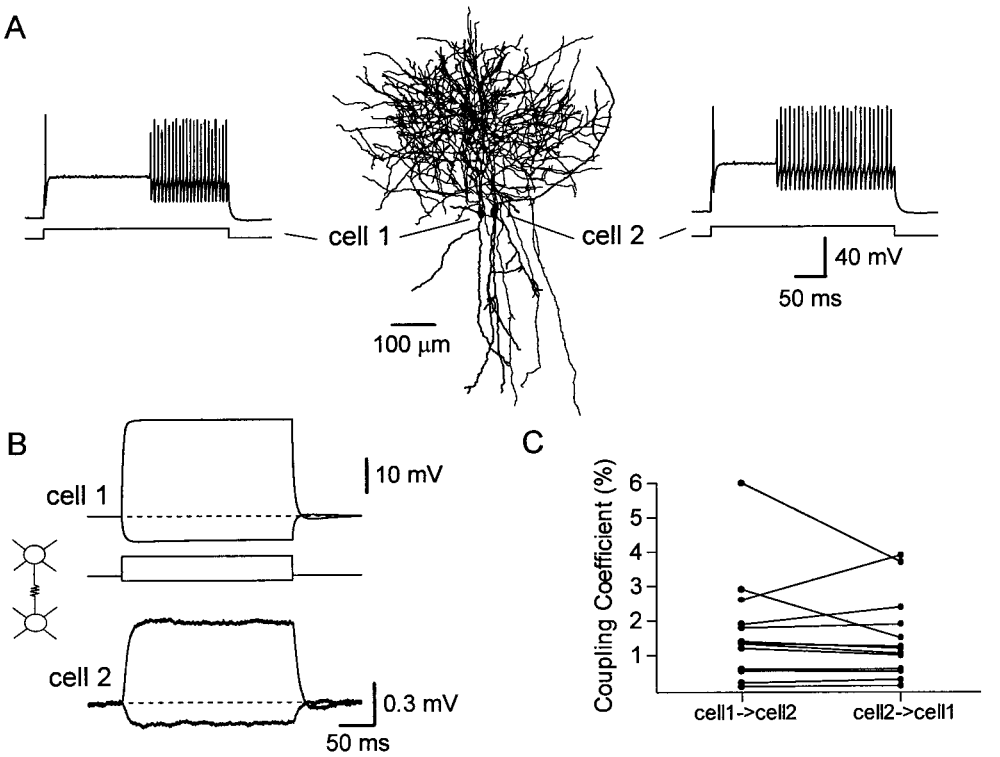

Fig. 2. (*A*) Neurolucida reconstruction of a pair of PV-FS cells simultaneously recorded in a slice from a 2-month-old mouse. The firing patterns of both cells in response to current injection (300 ms, 1 nA) are shown in the insets. (*B*) The injection of depolarizing (600-pA) or hyperpolarizing (150-pA) current in cell 1 simultaneously affected the membrane voltage of the noninjected cell 2. Step-coupling coefficient = 2.0%. Each trace is the average of 50 trials. Data are from the same pair illustrated in *A*. (*C*) Electrical coupling is bidirectional. Comparison of the step-coupling coefficient when current is injected in cell 1 versus cell 2 is shown.

ways bidirectional and had roughly equal magnitude in both directions. Because the input resistance of PV-FS cells was generally homogeneous, this suggests that the electrical junctions are usually located at similar electrotonic distances in both neurons. Assuming a model in which the cells are isopotential (26) we estimated that the coupling conductance between a pair of PV-FS cells was 0.203 ± 0.044 nS (range 0.013–0.586 nS, $n = 14$).

Next, we studied the efficacy of electrical synapses in transmitting presynaptic action potentials. When a presynaptic action potential was generated by a brief (2–3 ms) suprathreshold current injection, the electrical transmission of the presynaptic spike could be isolated by subtracting the postsynaptic response generated by a subthreshold injection (Fig. 3*A*). To examine the signal caused by an action potential in isolation, in other experiments the membrane of the presynaptic cell was depolarized to near threshold where spontaneous spikes were produced. These action potentials then were aligned, allowing the averaging of the postsynaptic responses. At an electrical connection, the action potential is transmitted as a biphasic signal: first, a brief depolarization (spikelet) reflecting the spike itself, and second, a slower hyperpolarization reflecting the presynaptic spike after

Table 1. Electrical and chemical connectivity among pairs of PV-FS cells

	Chemical (%)			Total (%)
	−	→	↔	
Electrical −	4 (17)	5 (22)	0 (0)	9 (39)
Electrical +	1 (4)	3 (13)	10 (44)	14 (61)
Total	5 (22)	8 (35)	10 (43)	23 (100)

Electrical −, absence of electrical connection; Electrical +, presence of electrical connection; Chemical, chemical connection; →, unidirectional chemical connection; ↔, reciprocal or bidirectional chemical connection.

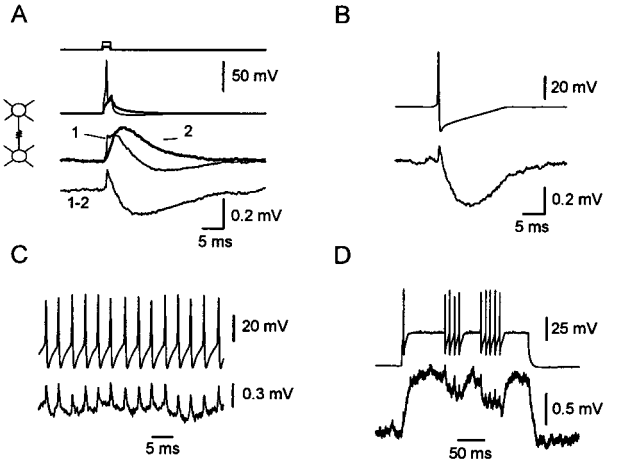

Fig. 3. Spike transmission through electrical synapses. (*A*) Spikelet obtained by subtracting supra- (1, thin traces) and subthreshold (2, thick traces) current injections in a pair of PV-FS cells connected only by electrical synapses. Step-coupling coefficient = 2.6%. Spike-coupling coefficient = 0.60%. (*B*) Isolated spikes were generated with near-threshold presynaptic injections. Spontaneous action potentials were aligned and averaged. Traces are the average of 17 trials. (3-month- and 2-week-old mouse). (*C*) Single traces showing spikelets transmitted in response to a discharge of presynaptic action potentials. Step-coupling coefficient = 3.7%. Spike, coupling coefficient = 0.94% (11-week-old mouse). (*D*) Brief trains of presynaptic action potentials result in a transient postsynaptic hyperpolarization. Single traces, data from *A*, *B*, and *D* are from same pair of cells.

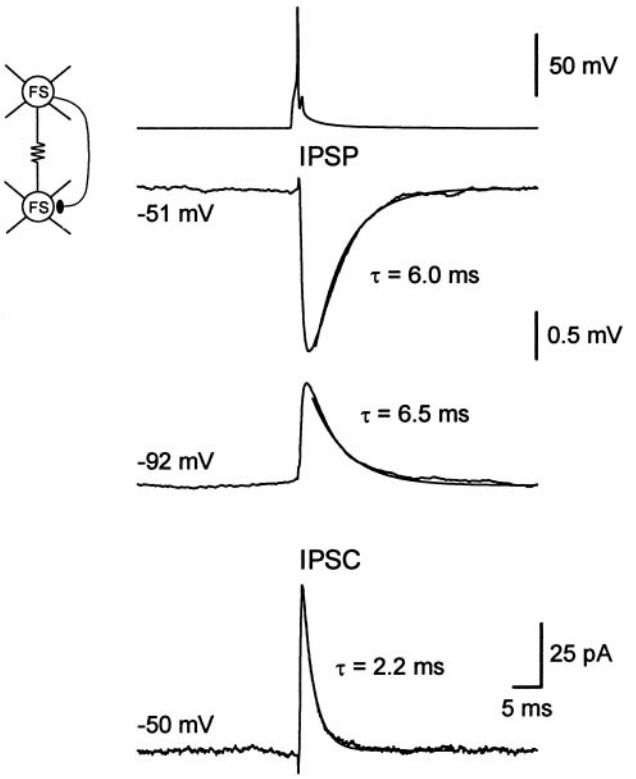

Fig. 4. Paired recording from two PV-FS cells (3 months and 2 weeks old) connected by both electrical and chemical synapses. IPSPs were recorded keeping the postsynaptic neuron under current-clamp at two different potentials (−51 and −92 mV). IPSC was recorded holding the postsynaptic neuron under voltage-clamp at −50 mV. Traces are the average of 50 trials. Step-coupling coefficient = 1.1%.

hyperpolarization (Fig. 3*B*). The delay between the peaks of the presynaptic spike and the postsynaptic spikelet was on average 0.26 ± 0.02 ms ($n = 10$). The average coupling coefficient for the spike (see *Materials and Methods*) was 0.51% ± 0.10% ($n = 9$), a value ≈3-fold smaller than that of the step-coupling coefficient. Individual spikes are transmitted during discharges of presynaptic spikes as brief depolarizations (Fig. 3*C*). However, as a result of the electrical transmission of the after-hyperpolarization potential, a train of presynaptic spikes can result in a relative postsynaptic hyperpolarization (Fig. 3*D*). The transmission of the after-hyperpolarization potential, similarly to GABA type A ($GABA_A$)-mediated inhibitory postsynaptic potentials (IPSPs), could contribute significantly to the detection of synchronous activity by networks of FS cells (27).

GABAergic Synapses Among PV-FS Cells. To study the connectivity via GABAergic synapses, we generated presynaptic action potentials with brief (2–3 ms) suprathreshold current injections and recorded the postsynaptic responses at two different membrane potentials. If the neurons were connected via chemical synapses, we observed a GABA-mediated hyperpolarizing IPSP at −50 mV that reversed its polarity and became depolarizing when the postsynaptic cell was kept at −90 mV (Fig. 4). Single-axon IPSPs between PV-FS cells were blocked by bath application of bicuculline methiodide (10 μM, $n = 2$, data not shown), indicating that they are mediated by $GABA_A$ receptors. We found that 78% of the pairs (18 of 23) were connected by GABAergic synapses (Fig. 5 and Table 1). The chemical connections were unidirectional in 8 pairs and bidirectional in another 10 pairs. In addition, 13 of the 14

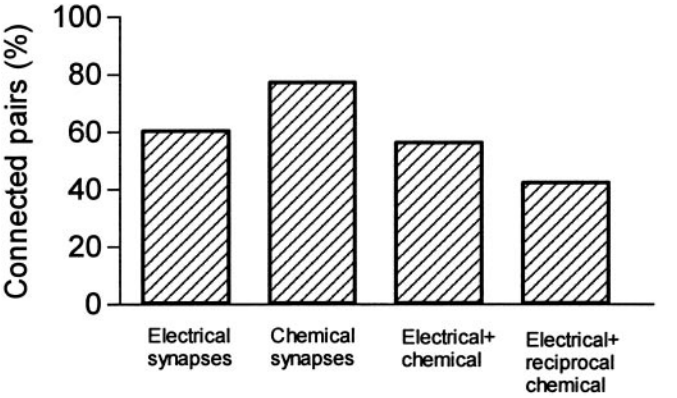

Fig. 5. Bar plot showing the percentage of recorded pairs of PV-FS cells connected by electrical and chemical synapses in adult mice.

electrically coupled pairs were also connected via chemical synapses in at least one direction. The 10 pairs bidirectionally connected via chemical synapses were electrically coupled (Figs. 5 and 6).

The mean peak amplitude of single-axon IPSPs at −50 mV was 0.72 ± 0.11 mV (range 0.1–1.7 mV, $n = 27$ pairs). The mean rise time (10–90%) was 0.89 ± 0.04 ms, and the mean delay between the peak of the presynaptic spike and the negative peak of the IPSP was 2.2 ± 0.08 ms. At a membrane potential of −50 mV, the single-axon IPSPs decayed with an exponential time course, the mean decay time constant of which was 5.9 ± 0.5 ms ($n = 24$, Fig. 4). When recorded at a membrane potential of −90 mV, the synaptic potential reversed its polarity and decayed with a mean time constant of 6.8 ± 0.7 ms ($n = 12$). This value was not significantly different from that obtained at −50 mV ($P > 0.3$). Thus, in contrast to the IPSPs at pyramidal neurons (28), the time course of the IPSPs among FS cells was not voltage-dependent.

The decay time course of inhibitory synaptic currents has been proposed to play an important role in determining the frequency at which GABAergic networks can synchronize their activity (14, 19). Slow GABA-mediated postsynaptic conductances result in

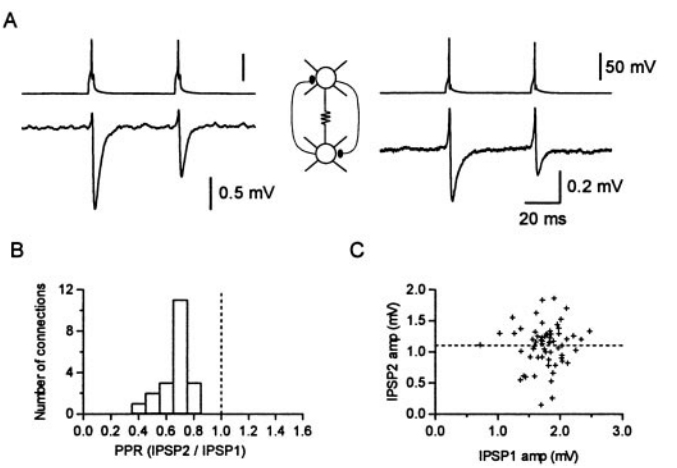

Fig. 6. (*A*) A pair of PV-FS cells electrically coupled and reciprocally connected through chemical connections. Step-coupling coefficient = 1.8 and 1.9%. Spike-coupling coefficient = 0.32 and 0.40% (2-month-old animal). (*B*) Histogram summarizing paired-pulse ratios (PPRs) from 24 connections. (*C*) Plot comparing the amplitude of IPSP2 versus IPSP1 for individual events ($R = 0.061$). The paired-pulse ratio in this connection was 0.61 (3-month- and 2-week-old animal).

low-frequency oscillations, whereas networks connected by faster IPSCs synchronize their activity at higher frequencies. The properties of the IPSCs were studied by keeping the postsynaptic cell under voltage-clamp (Fig. 4). At a holding potential of −50 mV, the average unitary IPSCs decayed exponentially, and the mean decay time constant was 2.6 ± 0.2 ms ($n = 8$ connections). We found that the mean peak amplitude of the unitary inhibitory synaptic currents was 23.9 ± 7.8 pA, and that the latency between the peak of the presynaptic spike and that of the IPSC was 1.1 ± 0.09 ms. The estimated unitary synaptic conductance was 797 pS. At a holding potential of −90 mV, the synaptic current became outward, but its decay kinetics ($\tau = 2.3 \pm 0.3$ ms) were similar to those of the IPSCs obtained at −50 mV. Lack of voltage dependence of IPSCs has been described previously at neocortical pyramidal neurons (28). In the hippocampus, however, IPSCs at principal cells have been reported to show a slower decay time course at depolarized potentials (29, 30).

Several studies have described developmental changes in the short-term plasticity of excitatory connections in the neocortex (31, 32) and inhibitory ones in the cerebellum (33). In all the cases, a switch from depression to facilitation was found by comparing slices from 3- versus 5-week-old animals. We examined frequency-dependent changes in single-axon IPSPs between PV-FS cells in slices from adult mice by measuring the paired-pulse ratio. We found that the average second IPSP was smaller than the first one when two presynaptic action potentials (50-ms interval) were generated. In 24 pairs, the ratio between the average IPSP2 and the average IPSP1 was 0.66% ± 0.02% (Fig. 6). Paired-pulse depression was observed in all the pairs we studied (Fig. 6*B*). We found that $GABA_A$ receptor-mediated synaptic transmission among FS cells showed short-term depression both in adult animals (34) as well as in young ones (7, 9, 20). Interestingly, when examining the trial-to-trial response variability, we found no significant correlation between the amplitudes of the second and the first IPSPs ($R = 0.05$, $n = 11$; Fig. 6*C*; ref. 35). Thus, although the average second IPSP was smaller than the average first IPSP, a relatively small individual second IPSP could be preceded by a relatively large or small individual first IPSP. This finding suggests that a mechanism different from transmitter depletion underlies paired-pulse depression in GABAergic synapses among FS cells.

Discussion

Our results indicate that in the adult neocortex, PV-FS cells can form an extensively interconnected network based on electrical and chemical synapses.

Electrical Synapses. Electron-microscopical observations (20, 36–38) and connexin 36 (Cx36) mRNA and immunohistochemistry (39–42) studies indicate that some GABAergic neurons are interconnected via gap junctions in the adult neocortex. Recent reports using paired recordings in slices from juvenile animals (2–4 weeks old) have demonstrated that GABAergic interneurons belonging to the same type, but not pyramidal neurons, are electrically coupled (refs. 7, 9, 20–23, and 43; for review see ref. 5). At this age, however, the neocortex is not mature. It has been suggested that synaptogenesis of the inhibitory system reaches adult values between 4 and 8 weeks postnatally (44). In addition, dye coupling rapidly declines in the second postnatal week (45, 46), and studies on Cx36 indicate that this protein could be expressed in both principal cells and interneurons in early postnatal development but primarily in interneurons in the adult (23, 39). Thus, it was important to directly demonstrate functional electrical coupling among GABAergic interneurons in the neocortex of adult animals.

Our results, obtained from adult animals ranging between 2 and 7 months old, show that electrical coupling among GABAergic PV cells is maintained in the adult neocortex. Interneuronal electrical coupling has also been demonstrated directly in the adult cerebellar cortex (47). The degree of connectivity via electrical synapses in adult slices, ≈60% of the pairs, was similar to that reported for juvenile rats (7, 9, 20) and mice (22). On the other hand, the strength of the electrical coupling among PV-FS cells in adult mice was relatively weak (1.5%). This value is smaller than that found in juvenile rats (3.8–7%; refs. 7, 9, and 20) and mice (6%; ref. 22). A reduction in the input resistance of PV-FS cells could contribute to this result. However, the input resistance of PV-FS cells in adult animals (89.2 ± 2.9 MΩ) was larger than that from young mice (70.8 ± 9.2 MΩ). In addition, it is possible that the dendrites and the electrotonic distance of electrical synapses are longer in adult mice than those in young animals. Finally, a reduction in the coupling coefficient could reflect a decrease in the coupling conductance, resulting from a smaller number of electrical junctions, fewer gap-junction channels per contact, or down-regulation of the conductance of individual gap-junction channels. We have estimated that the range of the coupling conductance was 0.13–0.58 nS, and the estimated average was 0.2 nS. In a recent modeling study, Traub *et al.* (24) found that networks of inhibitory neurons can generate "high synchrony" when the dendritic junctional conductance was ≈0.3 nS. Thus our findings suggest that electrical junctions in the adult neocortex could have an important effect on coherent activity of inhibitory neurons.

The role of inhibitory neurons in responding to the timing of sensory inputs in the cortex has been proposed as a mechanism determining the critical period (48). It has been suggested that maturation of neocortical inhibitory synapses is linked to the onset and termination of the developmental critical period (49, 50). Therefore, it is possible that a developmental decrease in the strength of electrical coupling may increase the threshold of activity required for activating groups of inhibitory neurons in adult animals and thus may be related to the termination of the critical period.

GABAergic Synapses. We found that the degree of connectivity among PV-FS cells via GABAergic synapses in the adult neocortex is 78% similar to that reported among FS cells in juvenile mice (22). We have found that unitary IPSCs among PV-FS cells in slices from adult mice decayed with a time constant of 2.6 ± 0.2 ms. This value is faster than that reported previously for IPSCs among pairs of GABAergic interneurons (basket cells) in the young rat neocortex (8.3 ms; ref. 20), indicating that $GABA_A$ receptor-mediated synaptic currents may exhibit faster decay kinetics in the adult than in the young neocortex. This faster IPSC decay kinetics may reflect different subunit composition of synaptic $GABA_A$ receptors in mature animals (51, 52). Fast-decaying IPSCs and a brief membrane time constant in adult PV-FS cells (3.8 versus 8 ms in FS cells from young rats) also resulted in $GABA_A$ receptor-mediated IPSPs with faster decay (5.9 ms; see also ref. 33) than that described in young rats (≈10 ms; ref. 7).

Functional Implications. It has been proposed that networks of GABAergic neurons and PV cells in particular are important in producing coherent high-frequency oscillations (10–12, 53–55) as well as detecting and promoting synchronous activity (27). These proposals critically depend on the properties of synaptic interactions among GABAergic neurons within the networks (14, 19, 24). Theoretical work has indicated that GABAergic connections may be sufficient to ensure coherent activity of inhibitory networks only under specific restrictions (17, 18, 24, 56). In addition, recent studies have shown that the loss of connexin 36, the major connexin underlying electrical coupling among interneurons, weakens synchronized network oscillations in brain slices (22, 23). On the other hand, the decay time course of inhibitory synaptic inputs has been proposed to play an

important role in determining the frequency at which GABAergic networks can synchronize their activity (14, 17, 19). Fast conductances of the synaptic connections between PV-FS cells may promote the generation of high-frequency oscillations (>60 Hz; refs. 14 and 19). Thus, the prominent level of GABAergic connectivity as well as the fast time course of the IPSCs among FS cells and their extensive electrical coupling demonstrated here would allow these networks to play a role in detecting and controlling spike timing in the adult neocortex.

We thank Hannah Monyer, Axel H. Meyer, and Novartis for the generous gift of the PV-EGFP transgenic mice, Zhiguo Chu and Veronika Zsiros for helpful discussions, and Rachel Hestrin for NEUROLUCIDA reconstructions. This work was supported by National Institutes of Health Grant EY12114.

1. Hendry, S. H., Schwark, H. D., Jones, E. G. & Yan, J. (1987) *J. Neurosci.* **7,** 1503–1519.
2. Meinecke, D. L. & Peters, A. (1987) *J. Comp. Neurol.* **261,** 388–404.
3. Kawaguchi, Y. & Kubota, Y. (1997) *Cereb. Cortex* **7,** 476–486.
4. Tamás, G., Buhl, E. H. & Somogyi, P. (1997) *J. Physiol. (London)* **500,** 715–738.
5. Galarreta, M. & Hestrin, S. (2001) *Nat. Rev. Neurosci.* **2,** 425–433.
6. Kawaguchi, Y. (1995) *J. Neurosci.* **15,** 2638–2655.
7. Galarreta, M. & Hestrin, S. (1999) *Nature (London)* **402,** 72–75.
8. Kawaguchi, Y. & Kubota, Y. (1993) *J. Neurophysiol.* **70,** 387–396.
9. Gibson, J. R., Beierlein, M. & Connors, B. W. (1999) *Nature (London)* **402,** 75–79.
10. Bragin, A., Jando, G., Nadasdy, Z., Hetke, J., Wise, K. & Buzsáki, G. (1995) *J. Neurosci.* **15,** 47–60.
11. Swadlow, H. A., Beloozerova, I. N. & Sirota, M. G. (1998) *J. Neurophysiol.* **79,** 567–582.
12. Jones, M. S., MacDonald, K. D., Choi, B., Dudek, F. E. & Barth, D. S. (2000) *J. Neurophysiol.* **84,** 1505–1518.
13. Cobb, S. R., Buhl, E. H., Halasy, K., Paulsen, O. & Somogyi, P. (1995) *Nature (London)* **378,** 75–78.
14. Whittington, M. A., Traub, R. D. & Jefferys, J. G. (1995) *Nature (London)* **373,** 612–615.
15. Lytton, W. W. & Sejnowski, T. J. (1991) *J. Neurophysiol.* **66,** 1059–1079.
16. Van Vreeswijk, C., Abbott, L. F. & Ermentrout, G. B. (1994) *J. Comput. Neurosci.* **1,** 313–321.
17. Wang, X. J. & Buzsáki, G. (1996) *J. Neurosci.* **16,** 6402–6413.
18. Rinzel, J., Terman, D., Wang, X. & Ermentrout, B. (1998) *Science* **279,** 1351–1355.
19. Bartos, M., Vida, I., Frotscher, M., Geiger, J. R. & Jonas, P. (2001) *J. Neurosci.* **21,** 2687–2698.
20. Tamás, G., Buhl, E. H., Lorincz, A. & Somogyi, P. (2000) *Nat. Neurosci.* **3,** 366–371.
21. Venance, L., Rozov, A., Blatow, M., Burnashev, N., Feldmeyer, D. & Monyer, H. (2000) *Proc. Natl. Acad. Sci. USA* **97,** 10260–10265.
22. Deans, M. R., Gibson, J. R., Sellitto, C., Connors, B. W. & Paul, D. L. (2001) *Neuron* **31,** 477–485.
23. Hormuzdi, S. G., Pais, I., LeBeau, F. E., Towers, S. K., Rozov, A., Buhl, E. H., Whittington, M. A. & Monyer, H. (2001) *Neuron* **31,** 487–495.
24. Traub, R. D., Kopell, N., Bibbig, A., Buhl, E. H., LeBeau, F. E. & Whittington, M. A. (2001) *J. Neurosci.* **21,** 9478–9486.
25. Meyer, A. H., Katona, I., Blatow, M., Rozov, A. & Monyer, H. (2002) *J. Neurosci.*, in press.
26. Bennett, M. V. (1977) in *Cellular Biology of Neurons*, ed. Kandel, E. R. (Williams & Wilkins, Baltimore), Vol. 1, pp. 357–416.
27. Galarreta, M. & Hestrin, S. (2001) *Science* **292,** 2295–2299.
28. Stuart, G. (1999) *Nat. Neurosci.* **2,** 144–150.
29. Collingridge, G. L., Gage, P. W. & Robertson, B. (1984) *J. Physiol. (London)* **356,** 551–564.
30. Otis, T. S. & Mody, I. (1992) *Neuroscience* **49,** 13–32.
31. Reyes, A. & Sakmann, B. (1999) *J. Neurosci.* **19,** 3827–3835.
32. Angulo, M. C., Staiger, J. F., Rossier, J. & Audinat, E. (1999) *J. Neurosci.* **19,** 1566–1576.
33. Pouzat, C. & Hestrin, S. (1997) *J. Neurosci.* **17,** 9104–9112.
34. Tamás, G., Somogyi, P. & Buhl, E. H. (1998) *J. Neurosci.* **18,** 4255–4270.
35. Kraushaar, U. & Jonas, P. (2000) *J. Neurosci.* **20,** 5594–5607.
36. Sloper, J. J. (1972) *Brain Res.* **44,** 641–646.
37. Sloper, J. J. & Powell, T. P. (1978) *Proc. R. Soc. London Ser. B* **203,** 39–47.
38. Peters, A. (1980) *Adv. Neurol.* **27,** 21–48.
39. Belluardo, N., Mudo, G., Trovato-Salinaro, A., Le Gurun, S., Charollais, A., Serre-Beinier, V., Amato, G., Haefliger, J. A., Meda, P. & Condorelli, D. F. (2000) *Brain Res.* **865,** 121–138.
40. Belluardo, N., Trovato-Salinaro, A., Mudo, G., Hurd, Y. L. & Condorelli, D. F. (1999) *J. Neurosci. Res.* **57,** 740–752.
41. Condorelli, D. F., Belluardo, N., Trovato-Salinaro, A. & Mudo, G. (2000) *Brain Res. Brain Res. Rev.* **32,** 72–85.
42. Priest, C. A., Thompson, A. J. & Keller, A. (2001) *Somatosens. Mot. Res.* **18,** 245–252.
43. Szabadics, J., Lorincz, A. & Tamás, G. (2001) *J. Neurosci.* **21,** 5824–5831.
44. Micheva, K. D. & Beaulieu, C. (1996) *J. Comp. Neurol.* **373,** 340–354.
45. Connors, B. W., Benardo, L. S. & Prince, D. A. (1983) *J. Neurosci.* **3,** 773–782.
46. Peinado, A., Yuste, R. & Katz, L. C. (1993) *Neuron* **10,** 103–114.
47. Mann-Metzer, P. & Yarom, Y. (1999) *J. Neurosci.* **19,** 3298–3306.
48. Feldman, D. E. (2000) *Nat. Neurosci.* **3,** 303–304.
49. Fagiolini, M. & Hensch, T. K. (2000) *Nature (London)* **404,** 183–186.
50. Huang, Z. J., Kirkwood, A., Pizzorusso, T., Porciatti, V., Morales, B., Bear, M. F., Maffei, L. & Tonegawa, S. (1999) *Cell* **98,** 739–755.
51. Dunning, D. D., Hoover, C. L., Soltesz, I., Smith, M. A. & O'Dowd, D. K. (1999) *J. Neurophysiol.* **82,** 3286–3297.
52. Hutcheon, B., Morley, P. & Poulter, M. O. (2000) *J. Physiol. (London)* **522,** 3–17.
53. Jefferys, J. G., Traub, R. D. & Whittington, M. A. (1996) *Trends Neurosci.* **19,** 202–208.
54. Hashimoto, I., Mashiko, T. & Imada, T. (1996) *Electroencephalogr. Clin. Neurophysiol.* **100,** 189–203.
55. Haueisen, J., Schack, B., Meier, T., Curio, G. & Okada, Y. (2001) *Clin. Neurophysiol.* **112,** 1316–1325.
56. Bush, P. & Sejnowski, T. (1996) *J. Comput. Neurosci.* **3,** 91–110.